Time-dependent deformation and craze initiation in PMMA: Volume effects

B. E. Read and G. D. Dean
Division of Materials Applications, National Physical Laboratory, Teddington, Middlesex, TW11 OLW, UK
(Received 16 March 1984)

As part of a study of long-term deformation and failure in glassy polymers, the time-dependent tensile compliance and lateral contraction ratio have been simultaneously determined for PMMA as a function of applied stress at room temperature. In the time range 10^2 to 10^6s, measurements of longitudinal and lateral strain were made using extensometers of novel design and a new optical interference technique was developed to serve as a check on lateral displacement data. At low stresses, the time-dependence of the tensile, shear and bulk compliance was derived over an extensive timescale range (10^{-8} to 10^6s) by combining the long-time data with transformed complex modulus and Poisson's ratio results. These data illustrated the large influence of the broad β retardation region on the room temperature creep behaviour and the onset of the glass-rubber or α region at long-times. With increasing stress a relatively large decrease in retardation times associated with the α process was principally responsible for the onset of non-linearity and resulted in an increased merging of the α and β regions. Stress-induced structural changes associated with this effect were indicated by a small initial positive contribution to the volumetric strain attributed to the partial erasing of previous physical ageing in the material. A subsequent decrease in volume might involve the mechanical enhancement of the original ageing. The substantial reduction in α retardation times with increasing stress was paralleled by a decrease in craze incubation times and this result is discussed in relation to craze initiation criteria based on considerations on non-linear viscoelastic response.

(Keywords: poly(methyl methacrylate); time-dependent compliances; α and β retardation processes; volumetric strain; physical ageing; craze initiation)

INTRODUCTION

In order to ensure the safe and efficient use of glassy thermoplastics, there is a continuing need for an improved understanding of their creep and crazing behaviour as a function of the applied stress state. The variation of strain with time at long periods after the application of a constant stress will usually involve conformational rearrangements of polymer chain segments arising from hindered rotations around main-chain bonds. This mechanism corresponds to the onset of the glass-rubber or primary (α) retardation region[1] and is considered to partly determine the linear and non-linear creep behaviour at low and high stresses respectively[2] and to participate in the phenomena of yielding and crazing[3]. However, the precise manner in which an applied stress influences the retardation times in the non-linear region is not quantitatively understood and this effect is complicated by a dependence on the non-equilibrium glassy structure as determined by the extent of previous physical ageing[2,4]. It should be emphasized that the term 'structure' in this paper refers to local details of the molecular conformation and/or packing and does not imply the existence of any long-range order in the amorphous materials. In the case of poly(methyl methacrylate) (PMMA), the behaviour at room temperature may be further complicated by the overlap between the α retardation region and the very broad secondary (β) retardation region. The degree of overlap could vary significantly with stress level in the non-linear region if the respective α and β retardation processes interact in a different way with the applied stress[4,5].

As part of an investigation of the origins of long-term creep and craze initiation in glassy polymers, giving emphasis to the possible role of volume changes, measurements have been made of both the longitudinal and lateral strains as a function of time and stress during the tensile creep of PMMA at room temperature. In the timescale range between about 70 and 10^6 s, the strains were determined following the application of stresses between 4.5 and 26.3 MN m^{-2} and times were recorded at which crazes were visually observed. Results at low stresses were obtained over an extended timescale range (10^{-8} to 10^6 s) by a combination of static and dynamic methods, allowing an assessment to be made of the effects of overlap between the α and β retardation regions. In this paper the measurement techniques will be outlined and the results discussed broadly in terms of the structural origins of non-linear creep and proposed viscoelastic criteria for the initiation of crazes.

SPECIFICATION OF TIME-DEPENDENT STRAINS AND COMPLIANCES

The application of a constant tensile stress σ along the x axis of an initially isotropic polymer strip gives rise to a time-dependent strain $\varepsilon_x(t)$ in the loading direction and to a lateral strain $\varepsilon_y(t)=\varepsilon_z(t)$. At small strains the time-dependent volume change $\Delta V(t)$ is given by

0032-3861/84/111679-08$03.00

$$\frac{\Delta V(t)}{V}=\varepsilon_x(t)+2\varepsilon_y(t)=\varepsilon_x(t)[1-2v_c(t)] \quad (1)$$

where V is the undeformed volume and $v_c(t)$ is the lateral contraction ratio $-\varepsilon_y(t)/\varepsilon_x(t)$, the subscript c being added to specify measurements during creep at constant stress[6].

In the range of low stresses for which the strains at any given time are each proportional to σ we may characterize the creep behaviour by the measured tensile compliance $D(t)=\varepsilon_x(t)/\sigma$ and $v_c(t)$ as functions of time. Contributions to the behaviour from the volume and shear components of the deformation may also be specified by the related bulk and shear compliance functions $B(t)$ and $J(t)$ respectively. Since the constant hydrostatic stress component of the applied tensile stress is of magnitude $\sigma/3$ we have

$$B(t)=\frac{3}{\sigma}\frac{\Delta V(t)}{V}=3D(t)[1-2v_c(t)] \quad (2)$$

Similarly from the shear strain $\varepsilon_x(t)-\varepsilon_y(t)$ and resolved constant shear stress component $\sigma/2$

$$J(t)=\frac{2}{\sigma}[\varepsilon_x(t)-\varepsilon_y(t)]=2D(t)[1+v_c(t)] \quad (3)$$

From equations (2) and (3) values of $B(t)$ and $J(t)$ may be evaluated from measured values of $D(t)$ and $v_c(t)$ as functions of time.

Above a certain stress level the time-dependent strains will no longer be proportional to stress, the deviations from linearity being generally dependent on time. In order to specify the non-linear creep behaviour, time-dependent compliances are evaluated according to the above relationships but they are now designated as *apparent* compliances (e.g. $D_a(t)$, $B_a(t)$) which of course depend on σ.

EXPERIMENTAL

Material

The PMMA employed in this investigation was a commercial grade (ICI Perspex) obtained in the form of cast sheets having a measured density of 1185 kg m^{-3}. For the long-term creep tests waisted specimens were cut from these sheets to ensure that crazing initiated in areas away from the stress concentrations around the clamped ends. The waisted sections were about 100 mm long, 10 mm wide and 6 mm thick and the machined sides were polished to enable accurate determinations of sample dimensions and strains and to minimize local stress concentrations. It should be added that the polishing was effected with the aid of jeweller's rouge and water which were not considered to have a pronounced influence on crazing. Since the earliest crazes tended nevertheless to nucleate on the machined and polished surfaces, these crazes were ignored and initiation times were determined for those crazes which nucleated on the original cast, unmachined surfaces. Rectangular strips or plates were employed for the short-time dynamic tests.

Measurement of tensile compliance and lateral contraction ratio at long times (10^2 s to 10^6 s)

Samples were gripped at each end within a tensile creep machine between a fixed lower clamp and an upper clamp to which loads up to 160 kg were applied via a 5:1 ratio lever arm. With the aid of a pneumatic piston device, the loads could be smoothly applied within about 2 s and the first strain measurements were automatically recorded 72 s (0.02 h) after loading. The creep machine was maintained at 23 ± 1°C and 50% relative humidity.

Measurements of sample extension in the longitudinal loading direction, and most measurements of the transverse sample contraction, were made with extensometers constructed in this laboratory and employing inductive displacement transducers. Some lateral contraction measurements were also made with a novel optical interference method to serve as a check on the long term stability of the transducer outputs.

The longitudinal extensometer (*Figure 1*) employed two inductive displacement transducers with high-precision linear bearings. The cores and bodies of the transducers were lightly clamped to the sample via knife edge mountings. These were set to span a known length of the sample with the aid of a slip gauge. A knife-edge radius of 0.25 mm was chosen to minimize any stress concentrations around the contact area with the sample which could influence local failure. With a gauge length of 50 mm, this length could be determined to much better than 1%. For the longitudinal extensometers, the transducers have been assembled without the core return spring in order to minimize resistance to sample movement. The two transducers were clamped to opposite faces of the sample so that their output could be averaged to correct for any slight sample bending.

The transverse extensometer (*Figure 2*) is held on the specimen by the force that the core return spring exerts on the sample. The total assembly weighs 30 g and the spring loading force of 120 g will give rise to a very small amount of transverse creep when the extensometer is attached. This is minimized by the insertion of a 10 mm^2 metal reaction pad placed between the transducer and sample and, in addition, the majority of transverse creep relaxation is allowed to occur before the application of the longitudinal stress. The transverse strain is inherently more difficult to measure accurately as the displacement is only about one tenth of that corresponding to the

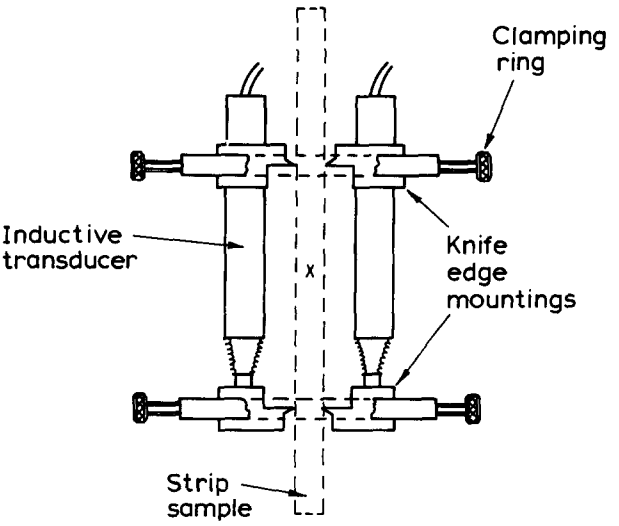

('x' marks position of transverse extensometer)

Figure 1 Longitudinal extensometer

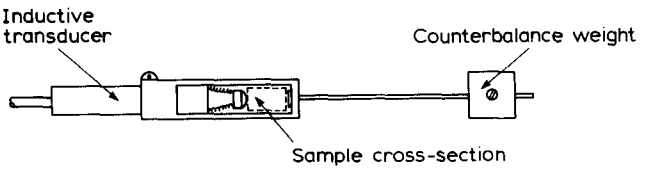

Figure 2 Transverse extensometer

longitudinal strain. Under ideal conditions the extensometers can measure displacements reproducibly to within 0.2 μm although other factors such as drift in the measuring electronics may act to lower this reproducibility in long term tests. The smoothness of the linear bearings in the transducers is of particular importance although an unsatisfactory bearing can be detected during calibration enabling the transducer to be rejected. The transducer outputs were automatically recorded on paper chart at various time intervals above 36 s between recordings.

The optical interference technique for measuring the lateral contractions is illustrated in *Figure 3*. Polarized light from a 1 mW, He-Ne, laser was passed through a low-powered convex lens and directed into the sample at near-normal incidence as a slowly diverging beam of about 1 mm diameter. Parts of this beam reflected from the respective front and back surfaces of the transparent specimen interfered to produce a series of light and dark fringes in the reflected beam which was received by a silicon photodiode detector. A negative lens before the detector served to expand the beam and separate the fringes further. The 1 mm aperture of the detector then allowed the maxima and minima in the fringe pattern to be accurately recorded owing to the relatively wide beam diameter (20 mm) and fringe spacing (4 to 5 mm) at this point. A 0.633 μm filter allowed the passage of the laser light but eliminated ambient radiation at other wavelengths which would otherwise saturate the detector. The detector output was fed to a high speed chart recorder for the purpose of counting the passage of fringes during the slow application of load to the sample and subsequent creep period.

With the optical technique, the observed fringe shift, or change in fringe order, corresponds to the change in optical path difference between the interfering reflected beams originating from the specimen deformation. Neglecting changes of refractive index with applied stress the change of sample thickness Δy would be related to the change of fringe order m by $\Delta y = m\lambda/2n$ where λ is the vacuum wavelength of the light and n the refractive index of the plastic. However, variations in refractive index with strain associated with changes in density will have a pronounced influence on the relationship between Δy and m. It is also necessary to take account of the anisotropy of refractive index or birefringence produced by the deformation and, in this context, polarized light was employed with the plane of polarization either parallel or perpendicular to the loading axis. The use of unpolarized light results in two overlapping fringe patterns produced by interference between the vertically polarized components of the reflected beams on the one hand and the horizontally polarized components on the other. Since the optical path lengths of the vertically and horizontally polarized components in the sample are different, owing to the birefringence, the maxima and minima in the overlapping patterns will not coincide.

Considering the variations of density, refractive index and birefringence due to an extension it can be shown that, to a good approximation,

$$\Delta y = \frac{\dfrac{m\lambda}{2n_0} - y_0\varepsilon_x\left[A - \dfrac{2K}{3n_0}\right]}{1-2A} \tag{4}$$

where n_0 and y_0 are the refractive index and thickness of the unextended sample and ε_x the longitudinal strain. The constant A equals the ratio of fractional refractive index change to fractional density change which, according to the Lorentz–Lorenz equation is given by

$$A = (n_0^2 - 1)(n_0^2 + 2)/6n_0^2$$

and the strain–optical coefficient K is written

$$K = (n_x - n_y)/\varepsilon_x$$

where $n_x - n_y$ is the birefringence, n_x and n_y being refractive indices for light polarized in the respective longitudinal and transverse directions. Equation (4) enables the determination of Δy and thus the lateral strain $\varepsilon_y = \Delta y/y_0$ from measurements of fringe shift m and ε_x if n_0, y_0 and K are known. For the PMMA used in the present investigation n_0 was found to be 1.480 ± 0.002 from the fringe shift caused by rotating a sample through known angles in a Michelson interferometer illuminated with laser light of wavelength $\lambda = 0.633$ μm. Birefringence measurements yielded a value of -1.2×10^{-2} for K which had a negligible time-dependence.

Determination of short-time compliances and lateral contraction ratios (10^{-8} s to 10 s)

Values of $D(t)$ and $v_c(t)$ were evaluated at very short times after loading from the transformation of dynamic mechanical data obtained over a wide frequency range. In this context we have employed the approximate formula given by Schwarzl and Struik[7]

$$D(0.48t) \approx D'(\omega) \qquad (t = 1/\omega) \tag{5}$$

where $D'(\omega)$, the tensile storage compliance at angular frequency ω, is related to the associated storage modulus $E'(\omega)$ and loss tangent $\tan\delta_E(\omega)$ by

$$D'(\omega) = [E'(1 + \tan^2\delta_E)]^{-1} \tag{6}$$

For the lateral contraction ratio we have assumed a similar approximation

$$v_c(0.48t) \approx v'(\omega) \qquad (t = 1/\omega) \tag{7}$$

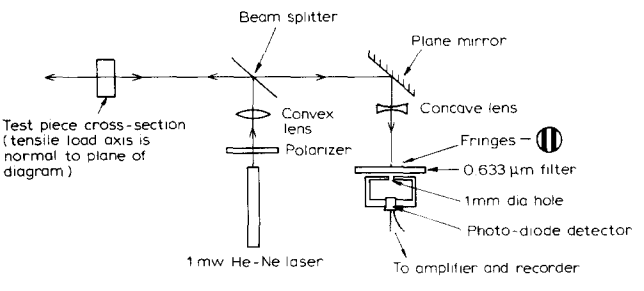

Figure 3 Optical arrangement for generating interference fringes

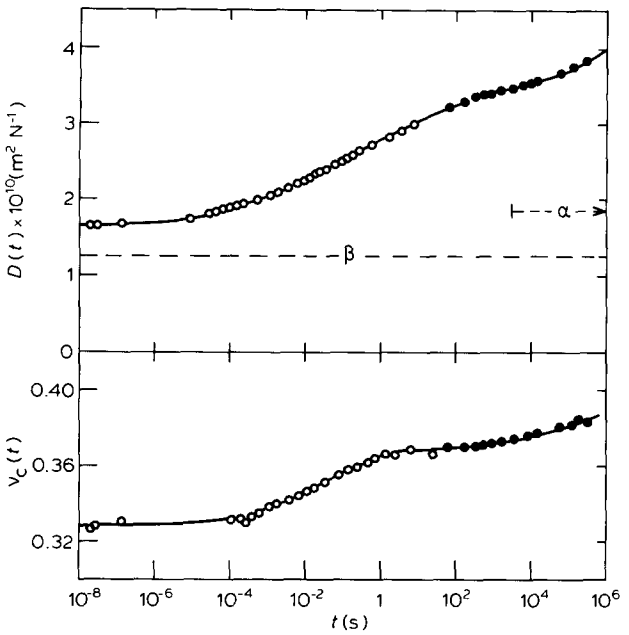

Figure 4 Time-dependence of the tensile compliance $D(t)$ and lateral contraction ratio $v_c(t)$ at low stress for PMMA at 23°C. (●), from direct strain measurements with a tensile stress of 9.07 MNm^{-2}; (○), derived from dynamic data at stress amplitudes below 1 MNm^{-2}. The β retardation region and onset of the α region is approximately indicated

where $v'(\omega)$ is the real part of the complex Poisson's ratio $v^* = v'(1 - i \tan \delta_v)$ defined previously[8].

The techniques employed for measuring the components of the complex modulus and Poisson's ratio have been fully described elsewhere[8-10]. For the present investigation most of the data were obtained by two techniques. In the frequency range 10^{-2} Hz to 10^3 Hz a forced non-resonance method was used involving measurements of the relative amplitudes and phases of the stress, longitudinal strain and lateral strain cycles respectively. For this purpose bi-directional strain gauges were bonded to tensile strips of the polymer which were time-harmonically deformed at a longitudinal strain amplitude of 0.02%. At frequencies between 5×10^5 Hz and 3.5×10^6 Hz measurements were made of the velocity and attenuation of both shear and longitudinal ultrasonic pulses transmitted through the material.

RESULTS

Behaviour at low stresses

Figure 4 shows the variation of $D(t)$ and $v_c(t)$ over about 13 decades of time at 23°C and illustrates the consistency of data obtained by the dynamic method at stress levels below 1 MN m^{-2} with the longer time static creep data at a stress of 9.07 MN m^{-2}. This result supports the validity of the transformation of dynamic data bearing in mind (as discussed below) that the stress of 9.07 MN m^{-2} is close to the maximum stress for which $\varepsilon_x(t)$ is proportional to σ, at least for times up to about 10^4 s.

It will be observed in *Figure 4* that $D(t)$ increases with time from a value of 1.6×10^{-10} m^2 N^{-1} at 10^{-8} s. The rate of increase of $D(t)$ exhibits a maximum at 10^{-1} s and subsequently decreases with time to a minimum around 10^4 s. This behaviour is characteristic of the extremely broad β retardation process which has a prominent influence on the creep data for PMMA at room temperature. However, the onset of the glass-rubber or α retardation process is reflected by a further increase in the rate of change of $D(t)$ at times above 10^4 s.

The β retardation process is also clearly evident in the time-dependence of $v_c(t)$ which increases (*Figure 4*) from a value of 0.33 at very short times to a value of 0.37 at 10 s. The pseudo plateau in the $v_c(t)$ curve in the region of 10 s to 10^3 s is more pronounced than that observed in the $D(t)$ curve owing to the somewhat narrower appearance of the β retardation and consequent smaller degree of overlap between the β and α retardation regions.

The derived time-dependence of $J(t)$ using equation (3) is closely similar to that found for $D(t)$, the substantial influence of the β process and onset of the α process being apparent in *Figure 5*. Also shown in *Figure 5* are values of the bulk compliance $B(t)$ evaluated on the basis of equation (2). The $B(t)$ curve levels off to a plateau in the long time region above 10^4 s, there being little apparent contribution to $B(t)$ from the α process at the times so far investigated.

Non-linear creep and crazing

In *Figure 6* the measured axial strains are plotted against time for stresses in the range 4.54 MN m^{-2} to 26.30 MN m^{-2}. Also indicated are the times for which crazes were observed for stresses of 15.80 MN m^{-2} and above. Although these times are shorter than those obtained for PMMA by Menges and Schmidt[11], a result which probably arises from differences between the grades of material, the observed decrease in craze induction time with increasing stress and strain is consistent with previous data for this and other polymers[11].

Figure 7 shows the time-dependence of the apparent tensile compliance ($D_a(t) = \varepsilon_x(t)/\sigma$) derived from the data in *Figure 6*. At the lowest stress, results have so far been obtained only for times up to about 10^4 s and within this timescale the $D_a(t)$ values at 4.54 and 9.07 MN m^{-2} are in close agreement. Departures from this substantially linear behaviour are observed at higher stresses by the increase of $D_a(t)$ with stress at any given time. However, the onset

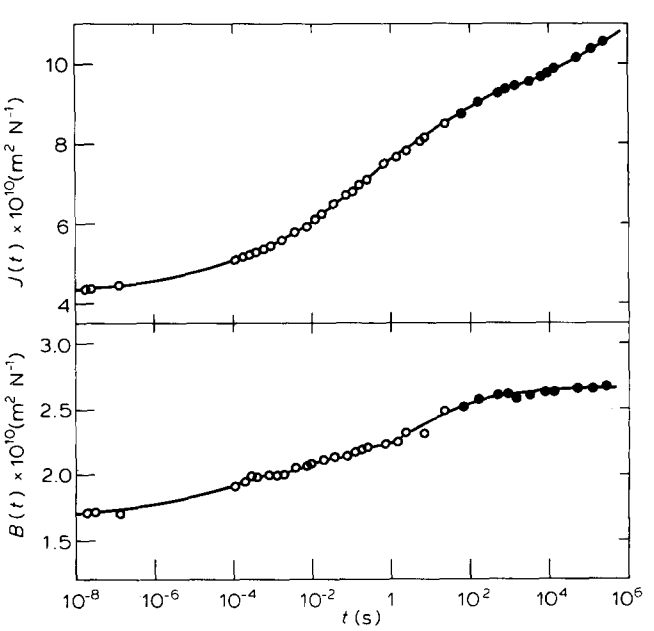

Figure 5 Shear compliance $J(t)$ and bulk compliance $B(t)$ as a function of time derived from the results of Figure 4

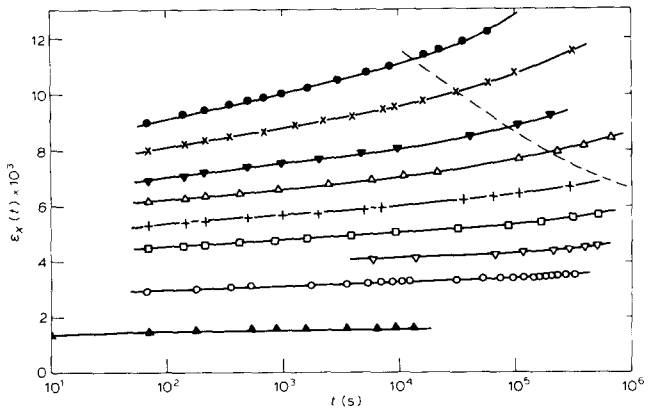

Figure 6 Longitudinal strain $\varepsilon_x(t)$ plotted against time for PMMA at 23°C at constant tensile stresses as follows: (▲), 4.54; (○), 9.07; (▽), 11.29; (□), 13.55; (+), 15.88; (△), 18.50; (▼), 20.61; (X), 23.65; (●), 26.30 MNm^{-2}. Times for the visual observation of crazes are indicated by the broken line (-----)

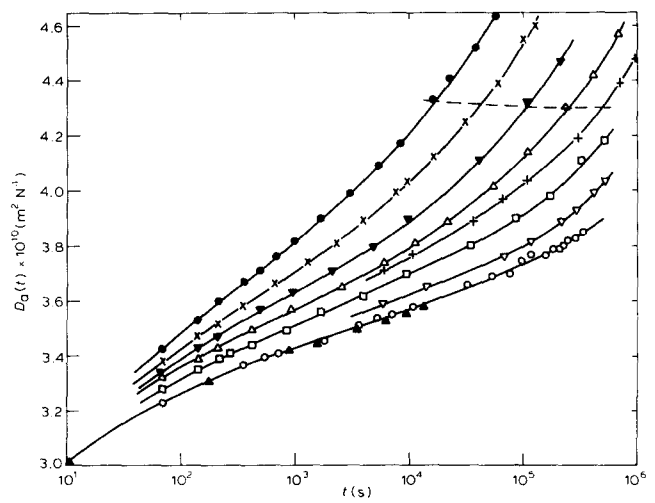

Figure 7 Time-dependence of the apparent tensile compliance $D_a(t)$ at various stresses for PMMA at 23°C. Point symbols and (- - -) as in *Figure 6*

of non-linearity may occur at lower stresses with increasing time and a more precise characterization of stress linearity limits requires further data in the low stress-long time region.

Some measured lateral contraction ratios are shown as a function of time in *Figure 8*. Comparative data obtained by the electrical extensometers and by the optical interference method suggest that $v_c(t)$ values were reproducible to within about $\pm 1\%$ for times up to 10^5 s. At longer times a somewhat lower accuracy was apparent in both methods of lateral strain measurement and the $v_c(t)$ values obtained electrically tended to be slightly higher than the optical values. This effect could not be accounted for by indentation of the sample by the transverse extensometer, which was negligible, and may involve electronic drift. The accuracy of the optical method is quite sensitive to values of ε_x which are required (equation (4)) owing to variations of the sample refractive index with strain. In order to eliminate this problem an optical extensometer is being developed which effectively replaces the sample surfaces by partially reflecting windows separated by a known air gap.

In *Figure 8* complete sets of data points are shown only for the applied stresses of 9.07 MN m^{-2} and 26.30 MN m^{-2}. At intermediate stress levels, selected points are shown to indicate the location of the curves at different stresses whilst avoiding the confusion due to the scatter of data at long times. For times greater than $10^{2.5}$ s it will be observed from *Figure 8* that $v_c(t)$ increases with increasing stress. A similar result was found by Benham and McCammond[12], although their $v_c(t)$ value of 0.40 at 10^2 is about 8% higher than our value.

The variation of volumetric strain with time and stress (*Figure 9*) was calculated from the data of *Figures 6* and *8* on the basis of equation (1). After an initial slight increase with time up to about $10^{2.5}$ s, subsequent variations of $\Delta V(t)/V$ are small, consistent with the overall time dependence of $B(t)$ in *Figure 5*. However, in the non-linear stress region $\Delta V(t)/V$ exhibits a significant decrease for times about 10^4 s.

The apparent bulk compliance $B_a(t) = 3\Delta V(t)/V\sigma$ is shown as a function of time and stress in *Figure 10*. For stresses up to 9.07 MN m^{-2}, $B_a(t)$ shows little variation with σ and increases with time toward a plateau value of 2.67×10^{-10} m^2 N^{-1} as illustrated also in *Figure 5*. At higher stresses $B_a(t)$ initially increases with t and σ, apart from some apparent inconsistency at intermediate stresses due to experimental errors around 3%, but subsequently passes through a broad maximum at times between about 10^3 and 10^4 s. The possibility that small electronic or temperature drifts may contribute toward the decrease in $\Delta V(t)/V$ and $B_a(t)$ at long times cannot however be discounted.

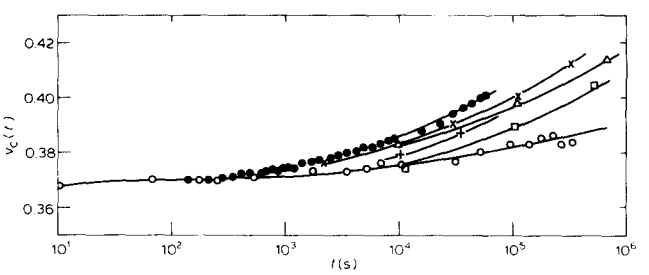

Figure 8 The lateral contraction ratio $v_c(t)$ as a function of time at different stress levels for PMMA at 23°C. Point symbols as in *Figure 6*

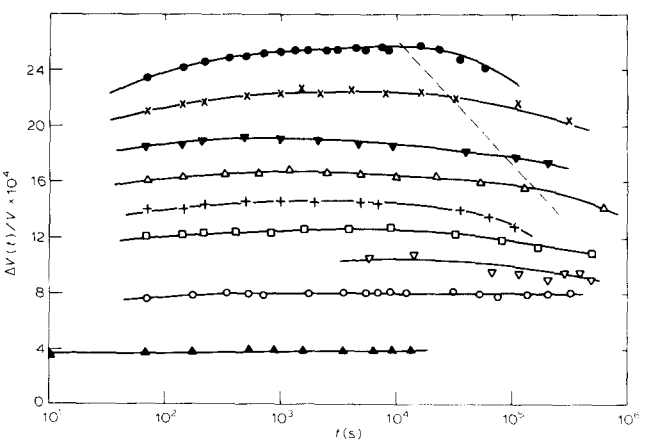

Figure 9 Variation of the volumetric strain $\Delta V(t)/V$ with time at different tensile stresses for PMMA at 23°C. Point symbols and (----) as in *Figure 6*

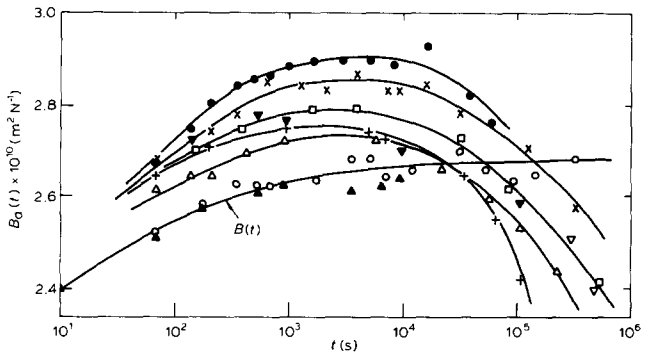

Figure 10 Time dependence of the apparent bulk compliance $B_a(t)$ calculated from the data of *Figure 9*

DISCUSSION

Creep and ageing phenomena

From *Figures 4* and *5* it is clear that the time-dependent deformation of PMMA at room temperature is considerably influenced by the broad β retardation process. This process is thought to involve rotations within side groups which may be coupled to local torsional displacements of the main polymer chain[10]. The increase in shear or tensile compliance at times greater than 10^3 s corresponds to the short-time tail of the glass-rubber or α retardation process which marks the onset of hindered rotations around main-chain bonds with consequent rearrangements in local chain conformation[1].

The non-linear behaviour illustrated in *Figure 7* may partly arise from an increase with stress of the equilibrium unrelaxed compliance of the α retardation process (or relaxed compliance of the β process) corresponding to a vertical shift of the creep curves. A more important factor appears to involve the shift of creep curves to shorter times resulting from a reduction in retardation times with increasing stress[2]. It is evident, however, that the curves cannot be superposed by horizontally shifting along the time axis, whether or not vertical shift factors are also applied. This result suggests that the shape of the retardation spectrum is changed by the applied stress in a manner corresponding to the increased merging of the α and β regions. Such an effect would arise if the stress caused a substantially larger decrease in retardation times associated with the α process than in those characteristic of the β process. It is well-known that physical ageing produces an increase in retardation times of the α process[2,13], and shape changes have been observed with increased ageing in both creep[4] and stress relaxation[14] curves for PMMA consistent with an increasing separation of the α and β regions. It thus appears that an applied stress in the non-linear region may yield a change in segmental mobility associated with the α process which is initially the reverse of that produced by physical ageing[2].

Although the time-dependences of $\Delta V(t)/V$ in *Figure 9* and of $B_a(t)$ in *Figure 10* are small, and subject to considerable magnification of experimental error, they could provide an important clue to the possible structural changes and mechanical ageing effects generated by the applied stress. In this context we first note that the non-equilibrium (quenched) glassy polymer had undergone prolonged ageing at room temperature prior to the present investigation. During this period, some volume reduction will have occurred by means of conformational rearrangements characterized by a broad distribution of volume retardation times[15,16]. Whilst some parts of the structure associated with relatively short volume retardation times may have thus approached their equilibrium states, most of the ageing will be exceedingly slow and the net volume will remain significantly higher than the equilibrium volume.

If a tensile stress in the linear range is applied to the polymer for times short compared with the α retardation times, local torsional displacements will occur around main-chain bonds but the sequences of rotational isomers which characterize the conformational structure will be unaffected. Under these conditions the volume increase $\Delta V(t)/V$ will result from the hydrostatic component of stress and will involve a net change in intermolecular spacing due to local elastic displacements about equilibrium positions. With higher applied stresses in the non-linear range the increased perturbations of the intra- and intermolecular force fields may also induce some changes in molecular conformation and packing. Neglecting a relatively small elastic contribution from the anharmonicity of the intermolecular force fields we assume that the non-linear part of $\Delta V(t)/V$,

$$\left(\frac{\Delta V(t)}{V}\right)_{nl} = \frac{\sigma}{3}\left[B_a(t) - B(t)\right] \tag{8}$$

arises mainly from these structural changes. Here $B_a(t)$ and the low-stress value $B(t)$ are measured at the same time.

At the highest stress so far applied (26.3 MN m^{-2}) the peak value of $B_a(t)$ in *Figure 10* is about 8% higher than the low-stress $B(t)$ value, yielding $(\Delta V(t)/V)_{nl} \approx 0.02\%$. This initial increase in $(\Delta V(t)/V)_{nl}$ is thought to arise mainly from stress-induced conformational changes which partially erase the original ageing of the polymer and are associated with the increased mobility of the α process. The subsequent decrease in $B_a(t)$ to values less than $B(t)$ corresponds to a negative $(\Delta V(t)/V)_{nl}$ and is indicative of a mechanical enhancement of the original ageing involving the longer volume retardation times. A thorough investigation of possible long-term sources of error is being undertaken in an attempt to confirm this suggestion.

The question arises as to whether the hydrostatic or shear component of the stress field is mainly responsible for the structural effects. As discussed by Struik[2], shear creep compliance curves, obtained from torsion tests in the absence of a hydrostatic stress component, also shift to shorter times with increasing shear stress. Similar shifts, although somewhat smaller in magnitude, are also observed from uniaxial compression tests[12] in which the isotropic compressive stress component produces a net contraction or negative $\Delta V(t)/V$. Furthermore a small *dilational* contribution to the volumetric strain, resembling our $(\Delta V(t)/V)_{nl}$, has been observed during the non-linear uniaxial compression of PMMA[17] whereas under hydrostatic compression[18] the volumetric strain is essentially proportional to hydrostatic stress up to 50 NM m^{-2}. These results indicate that the shear stress may be largely responsible for $(\Delta V(t)/V)_{nl}$ and the proposed structural changes.

The effects discussed above may be considered in terms of the influence of stress in generating an initial increase and subsequent decrease in 'free-volume' which may be

associated with the values of $(\Delta V(t)/V)_{n1}$ but *not* with the total $\Delta V(t)/V$. According to Robertson's theory of plasticity[19], the shear stress component alters the energy difference between the rotational isomeric states and the initial structural changes involve a transient increase in the number of high-energy conformations. The temporary structure resembles an equilibrium structure characteristic of a higher temperature with enhanced semgnetal mobility, and a transient volume increase is predicted which might be related to the peak value of $(\Delta V(t)/V)_{n1}$. Attempts are currently being made to assess the ability of the above models to quantitatively account for the stress-dependence of retardation times. These analyses, including a proposed method for separating the contributions to the creep data from the respective α and β retardation processes, will be reported subsequently[20].

It should finally be mentioned that the apparent maxima in volume during the tensile creep resemble the volume relaxation peaks, discussed by Kovacs[15] and by Struik[2], which are found after heating (to temperatures below T_g) samples of glassy polymers which had been previously quenched and stored for extended periods. This resemblance exemplifies the possible similarity in structural changes produced by the application of high stress and by increases in temperature.

Criteria for crazing

Although the detailed mechanisms of craze initiation are not well understood, it is widely considered that the local regions of voided, oriented polymer which constitute the craze structures result from the generation, accumulation and plastic expansion of cavities within the material[21-23]. Various elastic criteria for the initiation of crazes have been proposed, demonstrating the need for a dilational stress together with a stress bias[24] or shear stress, but the precise influence of the different stress components on the local molecuar mobility, cavity formation and molecular orientation is unclear. It has been recognized for some time that these inhomogeneous deformation processes are time-dependent and probably related to the non-linear creep deformation during constant load tests. From the results in *Figure 7* it is evident that the α retardation process is involved and that the retardation times and craze incubation times are similarly reduced by increases in the level of applied stress.

The results of the present investigation are also relevant to some recently proposed viscoelastic crazing criteria. Brüller[25] has found that, under a constant tensile stress σ, crazes become visible when the 'crazing incubation energy'

$$W_c = \sigma(\varepsilon_c - \varepsilon_{sp}) \tag{9}$$

attains a constant value. Here ε_c is the total strain $(\varepsilon_x(t))$ when crazes become visible and ε_{sp} is the 'quasi-spontaneous' strain existing immediately after the load application. W_c is thus the time-dependent energy per unit volume supplied to the polymer after the initial loading, part of the energy being stored within the material and part dissipated. Recognizing the difficulties associated with the determination of ε_{sp}, Brüller obtained values for PMMA by extrapolating creep curves to the vicinity of the loading times (1–2 s). The ε_{sp} values ranged from about 0.6% at $\sigma = 20$ MN m^{-2} to 2.2% at $\sigma = 50$ MN m^{-2} corresponding to compliance values around 3.0×10^{-10} and 4.5×10^{-10} m^2 N^{-1} respectively. It follows from *Figures 4* and *7* that during loading at 20 MN m^{-2}, relaxation will have occurred involving an appreciable portion of the β process, whilst at 50 MN m^{-2} a larger amount of relaxation, involving the α and β processes, would have taken place during the loading phase.

Assuming that craze initiation involves molecular motions associated either with the α process or with a combination of α and β mechanisms, it is instructive to consider the values of W_c obtained by the successive identification of ε_{sp} with the limiting unrelaxed strains $\varepsilon_{u\alpha}$ and $\varepsilon_{u\beta}$ of the respective α and β processes. After separating contributions to our creep curves from the α and β regions[20] we have estimated that, with increasing stress from 15.88 to 26.30 MN m^{-2}, $\varepsilon_c - \varepsilon_{u\alpha}$ increases from 0.12 to 0.17% and $\varepsilon_c - \varepsilon_{u\beta}$ increases from 0.43 to 0.68%. Hence if relaxation effects during the loading were accounted for, or if loads could be applied sufficiently rapidly to avoid relaxation during the loading period, it appears that the 'viscoelastic' energy W_c supplied for the incubation of crazing would increase with applied stress.

The estimated increases in $\varepsilon_c - \varepsilon_{u\alpha}$ and $\varepsilon_c - \varepsilon_{u\beta}$ with increasing stress also seem inconsistent with the constant 'inelastic strain' criterion proposed by Wright[26]. Furthermore, the crazes were not observed at a given value of volumetric strain (*Figure 9*) or of the increment $(\Delta V(t)/V)_{n1}$. It should also be noted in this context that no abrupt volume increases were observed which might be associated with crazing (cavitation), the volume changes being apparently dominated by the molecular relaxation and physical ageing effects.

The present data seem more consistent with a crazing criterion based on an approximate constancy of a compliance increment $((\varepsilon_c - \varepsilon_{u\alpha})/\sigma \approx 7 \times 10^{-11}$ m^2 N^{-1} or $(\varepsilon_c - \varepsilon_{u\beta})/\sigma \approx 2.6 \times 10^{-10}$ m^2 N^{-1}) rather than a constant increment of energy or strain. It should be emphasized, however, that the inherently large scatter in the observed craze incubation times and the breadth of overlapping retardation spectra cause considerable uncertainty in assessing the proposed criteria. Despite these difficulties it seems that those stress-induced structural changes considered to result in a reduction of retardation times also serve to decrease the craze initiation times. Since crazing is observed after only a small overall proportion of the α retardation mechanism has been effective, corresponding to the short time tail of the α region, stress-concentrating defects or local variations in structure seem necessary to account for the local large-scale molecular rearrangements apparently necessary in craze formation.

CONCLUSIONS

Simultaneous measurements of the time-dependent tensile compliance and lateral contraction ratio for glassy polymers can provide important data relevant to the retardation mechanisms and mechanical ageing effects which occur subsequent to the application of constant loads.

Results obtained at low stress levels over about 14 decades of timescale exemplify the prominent role of the β retardation process on the room temperature creep behaviour of PMMA, and the onset of the α process at long times after loading.

The onset of non-linear viscoelastic behaviour with increasing stress is largely determined by decreases in the

retardation times of the α process. The failure to superpose creep curves obtained at different stresses by simple horizontal and vertical shifts is ascribed to a relatively small stress-dependence of the β retardation times and consequent increased merging of the α and β retardation regions. A small non-linear contribution to the net time-dependent volume change is thought to reflect stress-induced conformational changes connected with the initial erasing and subsequent enhancement of previous physical ageing.

A decrease in craze incubation times with increasing stress correlates approximately with the increased segmental mobility associated with the α retardation process. The present data are not fully consistent with proposed criteria based on a constant viscoelastic energy input or constant inelastic (tensile or volumetric) strain, the craze initiation times appearing to correlate more closely with the level of time-dependent compliance.

ACKNOWLEDGEMENTS

The authors wish to thank Mr J. C. Duncan and Miss S. Golding for assistance with the construction of apparatus and creep measurements.

REFERENCES

1 McCrum, N. G., Read, B. E. and Williams, G. 'Anelastic and Dielectric Effects in Polymeric Solids', Wiley, London and New York, 1967
2 Struik, L. C. E. 'Physical Ageing in Amorphous Polymers and Other Materials', Elsevier, Amsterdam, 1978
3 Ward, I. M. 'Mechanical Properties of Solid Polymers', Wiley–Interscience, London, 1971
4 Myers, F. A., Cama, F. C. and Sternstein, S. S. *Ann. N.Y. Acad. Sci.* 1976, **279**, 94
5 Koppelmann, J., Hirnböck, R., Leder, H. and Royer, F. *Colloid Polym. Sci.* 1980, **258**, 9
6 Theocaris, P. S. *Polymer* 1979, **20**, 1149
7 Schwarzl, F. R. and Struik, L. C. E. *Adv. Mol. Relaxation Processes* 1968, **1**, 201
8 Read, B. E. and Dean, G. D. 'The Determination of Dynamic Properties of Polymers and Composites', Adam Hilger Ltd., Bristol, 1978
9 Read, B. E. and Duncan, J. C. 'Polymer Testing', Applied Science Publishers, 1981, **2**, 135
10 Read, B. E. *Polymer* 1981, **22**, 1580
11 Menges, G. and Schmidt, H. *Plast. Polym.* 1970, **38**, 13
12 Benham, P. P. and McCammond, D. *Plast. Polym.* 1971, **39**, 130
13 Cizmecioglu, M., Fedors, R. F., Hong, S. D. and Moacanin, J. *Polym. Eng. Sci.* 1981, **21**, 940
14 McKenna, G. B. and Kovacs, A. J. *Am. Chem. Soc. Polym. Prepr.* 1983, **24**, No. 2, 100
15 Kovacs, A. J., Aklonis, J. J., Hutchinson, J. M. and Ramos, A. R. *J. Polym. Sci.* 1979, **17**, 1097
16 Hutchinson, J. M. and Bucknall, C. B. *Polym. Eng. Sci.* 1980, **20**, 173
17 Whitney, W. and Andrews, R. D. *J. Polym. Sci. C* 1967, **16**, 2981
18 Mallon, P. J. and Benham, P. P. *Plast. Polym.* 1972, **40**, 77
19 Robertson, R. E. *J. Chem. Phys.* 1966, **44**, 3950
20 Read, B. E. and Dean, G. D. to be published
21 Rabinowitz, S. and Beardmore, P. Critical Reviews in Macromol. Sci. 1972, **1**, CRC Press, Chemical Rubber Co., Cleveland, Ohio
22 Kambour, R. P. *J. Polym. Sci., Macromol. Rev.* 1973, **7**, 1
23 Argon, A. S. *J. Macromol. Sci. Phys.* 1973, **B8(3–4)**, 573
24 Sternstein, S. S. and Ongchin, L. *Am. Chem. Soc. Polym. Prepr.* 1969, **10**, 1117
25 Brüller, O. S. *Polymer* 1978, **19**, 1195
26 Wright, D. C. *Br. Polym. J.* 1978, **10**, 60